INTERNATIONAL JOURNAL OF INTEGRATED ENGINEERING
ISSN: 2229-838X e-ISSN: 2600-7916

IJIE

Vol. 16 No. 1 (2024) 394-410
https://publisher.uthm.edu.my/ojs/index.php/ijie

# Prediction of Storm Surges in the East Coast of Peninsular Malaysia in Response to Climate Change

**Nurdiyana Nabilah Rosli[1*], Hee-Min Teh[1], Soo-Youl Kim[2]**

[1] *Department of Civil and Environmental Engineering*
*Universiti Teknologi PETRONAS, 32610 Seri Iskandar, Perak, MALAYSIA*
[2] *Department of Civil Environmental Engineering and Architecture*
*Kumamoto University, Kurokami South Campus, 860-0862, JAPAN*

*Corresponding Author: nurdiyana_20001807@utp.edu.my
DOI: https://doi.org/10.30880/ijie.2024.16.01.033

**Article Info**

Received: 17 December 2023
Accepted: 22 May 2024
Available online: 30 June 2024

**Keywords**

Climate change, future climate database, numerical assessment, storm surge level

**Abstract**

This study employed the MIKE 21HD modeling framework, integrating data from the future climate database, "Policy Decision Making for Future Climate Change (d4PDF)" on selected critical ensembles to investigate the impact of climate change on storm surge height (SSH) along the East Coast of Peninsular Malaysia during the Northeast Monsoon season. Three scenarios, including past-historical data, future climate with a 2°C increment (+2K), and future climate with a 4°C increment (+4K), were analyzed. The study had validated model accuracy through root mean square error (RMSE), demonstrating alignment with observed data. Results indicated a correlation between temperature increase and storm surge height (SSH), with higher temperature scenarios leading to more severe surge outcomes. The analysis identified the Future +4K scenarios as yielding the most critical SSH across all stations, with recorded SSH at Kuala Pahang (SSHmax = 1.379 m), Chendering (SSHmax = 1.344 m), Geting (SSHmax = 1.251 m), and Tanjung Sedili (SSHmax = 1.251 m) stations. Considering the findings, it was recommended to reassess the baseline provision for coastal engineering projects, suggesting a storm surge resilience design exceeding the observed maximum. The utilization of d4PDF data in this study laid the groundwork for targeted strategies to mitigate the impacts of climate-induced storm surges in vulnerable coastal regions.

## 1. Introduction

Leading researchers from various fields of study, through their comprehensive and in-depth studies on recorded climate data around the world, have manifested that worldwide climate is changing [1]. Its profound impacts are evident across the globe, including in Malaysia, where changes in temperature and precipitation patterns are reshaping the country's environmental landscape and threaten to exacerbate poverty and inequality for low-income earners especially in localities that are vulnerable to flooding and drought [2]. This is proven and consistent with findings from [3]-[6] which claim the vulnerability of neighboring countries in the Asia region based on forecasted intensity of precipitation under the influence of climate change.

The analysis from IPCC Fifth Assessment Report (AR5) has reported a peak increment of global mean surface temperature at 3.11°C for RCP8.5 (which is the highest emissions pathway) and 0.8°C for RCP2.6 (which is the lowest emissions pathway) by the year 2090s [7], as shown in Fig. 1. An important implication of climate change is the phenomenon of sea level rise as a result of thermal expansion and continuous ice cap melting [8]. In Malaysia, it was supported by a finding from research [9] using linear trend analysis and assimilation of 7 Coupled

Atmospheric-Oceanic General Circulation Model (AOCGM), highlighting that the regional rise for Malaysia's mean SLR would be higher than 3.1 mm/year (between 2.7 to 7.0 mm/year), resulting in a higher risk of low-lying areas to be inundated. On other hand, a study in 2010 on extreme wind speeds using graphical method in Peninsular Malaysia claimed that over a long period (50 years onwards), a sharp increase in the trend was expected [10]. The combination of warmer ocean, SLR and extreme wind would impact the behavior of storm surge, especially its heights.

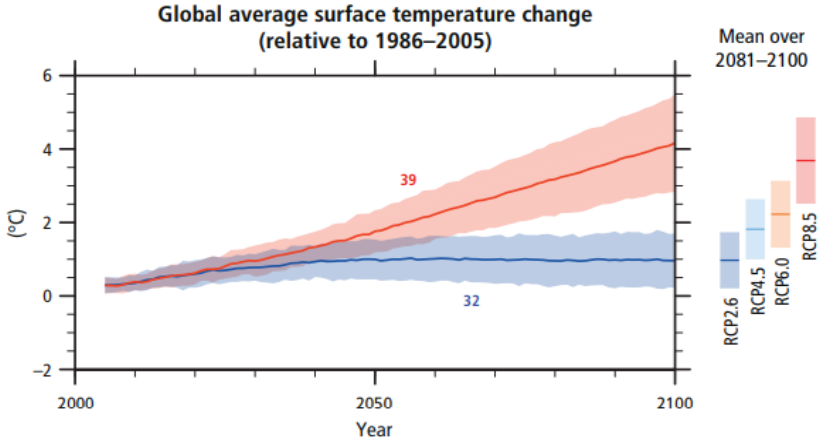


**Fig. 1** *Global average surface temperature change [7]*

Storm surges are perturbations in sea surface level caused by either storms, hurricanes, typhoons, and tropical cyclones which has the pivotal key element of having the high intensity winds (wind drag) along with the atmospheric forcing, and pressure drops [11]. Storm surge level can be determined through time series by finding the differences between predicted tide level and observed sea surface level as it coincides with astronomical tides. Storm surge itself is dangerous and in conjunction with high tides at wide-shallow shelf sea, the impact would be amplified. Storms with high wind intensity push the water into shore causing death, significant property damage, changes in ecosystem and landscape and coastal erosion and destruction at the vulnerable areas. By studying the behavior of storm surge and forecasting the event for a long return period, risk mitigation planning can be prepared to reduce the cost of the damages. Besides, the process to evacuate the population living near the coastal site can be conducted efficiently with proper planning. Aside from that, climate change phenomenon is also contributing to the altered behavior of the wind as well as sea level rise that influence the characteristics of the storm surge.
While the destruction come with an excruciating and devastating price, the study of storm surge events in Malaysia are still considered as low although this country is 29$^{th}$ longest water bounded - surrounded by a total of 4,800 kilometres of coastline. Thus, this research intended to conduct the assessment of storm surges in Malaysian seas in response to climate change which will be forcing the scenarios of Database for Policy Decision Making for Future Climate Change (d4PDF). The objectives of this study are: (i) To simulate storm surge scenarios considering 2K and 4K global mean temperature increased compared to pre-industrial levels and (ii) to project the storm surge heights (SSH) in the East Coast of Peninsular Malaysia, corresponding to climate change impact.

## 2. Illustrations Datasets and Procedures

### 2.1 Overview on Future Climate Database d4PDF

The Database for Policy Decision-making for Future Climate Change (d4PDF) is a comprehensive and valuable resource developed by the Meteorological Research Institute (MRI) in Japan. It is part of the Coupled Model Intercomparison Project 5 (CMIP5) which provides a collection of climate simulations covering the period from 1951 to 2100. CMIP5 contributed to the assessment reports of the Intergovernmental Panel on Climate Change (IPCC) released in 2013 to 2014, offering valuable insights into future climate change scenarios and their potential impacts. It is important to note that the dataset had been simulated based on four different scenarios of greenhouse gas emissions known as Representative Concentration Pathways (RCPs): RCP 2.6, RCP 4.5, RCP 6.0 and RCP 8.5. Whereas RCP 2.6 represents a future with ambitious emissions reductions, aiming to limit global warming to well below 2°C. While, RCP 4.5 and RCP 6.0 correspond to moderate and limited mitigation efforts, respectively, resulting in higher levels of warming, and RCP 8.5 represents a high-emission pathway, leading to significantly warmer temperatures by the end of the century.

Within the d4PDF database, the focus lies on the regional climate dynamics captured by the General Circulation Models (GCMs). GCM is initially divided into two components, Atmospheric General Circulation Models (AGCMs) and Ocean General Circulation Models (OGCMs). AGCMs capture atmospheric processes like

temperature, humidity, wind patterns, and precipitation but do not explicitly include the full complexity of the oceans. Whereas OGCMs simulate important processes like ocean circulation, heat transport, and interaction with the atmosphere. This study focused on one of the AGCM subsets, namely the Meteorological Research Institute Coupled General Circulation Model version 3 (MRI-CGCM3) [12]. It includes simulations at both global and regional scales, with horizontal resolutions of 60 km and 20 km, respectively. The model takes into account a wide range of factors, featuring (i) the atmospheric component based on the Nonhydrostatic Icosahedral Atmospheric Model (NICAM), which employs a high-resolution icosahedral grid for enhanced accuracy in simulating atmospheric processes (110 km horizontal resolution, 80 vertical levels), (ii) the ocean component utilizes the Modular Ocean Model version 4 (MOM4) with a horizontal resolution of approximately 0.5 degrees and 45 vertical levels, (iii) the land surface component incorporates representations of vegetation, soil moisture, and other biophysical processes impacting energy and water exchange, (iv) and the sea ice component employs a dynamic sea ice model to simulate growth and retreat based on temperature and ocean changes. The model further includes a module simulating interactions between atmospheric aerosols and climate, influencing Earth's radiative balance and climate dynamics. This subset is selected as it specifically designed to cover the Japanese and Korean Peninsulas, as well as parts of the Asian continent including Malaysia, providing valuable insights into the regional climate changes and their potential impacts. For the past five years, Japanese researchers have actively led the usage of this database for various studies related to the ocean [13]-[16].

Multiple sets of future climate simulations are available, with different levels of global mean surface air temperature increases. These include simulations with a 4K, 2K, and 1.5K temperature increase relative to preindustrial levels which typically referred as time before Industrial Revolution around mid-19th century. These scenarios represent different warming levels and provide insights into the potential climate changes associated with different levels of global warming. In the context of this study, the focus is on the 2K and 4K future climate scenarios. These scenarios represent temperature increases of 2 and 4 degrees Celsius above preindustrial levels, respectively.

The d4PDF datasets offer the output in the form of super-various ensembles. An ensemble refers to a collection of climate model simulations that capture different possible outcomes of future climate conditions. Each ensemble member represents a unique realization of the climate system, incorporating variations in initial conditions, parameterizations, or model configurations. By running multiple ensemble members, the d4PDF database accounts for uncertainties and provides a range of possible climate projections [17]. For the historical and non-warming simulations, there are 100 ensemble members available for each component. As for the future scenarios 4K consists of 90 ensemble members from year 2051 to 2110, whereas 2K consists of 54 ensemble members from year 2031 to 2090.

The datasets from d4PDF database are stored in binary format and require conversion and preliminary study to understand the data structure. Unlike conventional user-friendly interfaces, working with d4PDF necessitates a familiarity with coding practices to extract meaningful insights. Data conversion could be done through MATLAB scripting by utilizing fread function to read the binary data, the raw information then underwent a crucial transformation into a structured 3D matrix. Each dimension of this matrix was assigned to represent specific aspects of the climate data, such as time, latitude, and longitude. This reorganization was fundamental for subsequent analyses and facilitated the gridded interpolation process before it could be imported into MIKE 21HD.

## 2.2 Research Area

Strategically positioned in Southeast Asia, Malaysia boasts a diverse and extensive coastline spanning approximately 4,675 kilometers along the South China Sea (SCS), Gulf of Thailand (GoT), and the Straits of Malacca as shown in Fig. 2. This region undergoes seasonal prevailing winds, commonly referred to as the monsoon. The monsoon in Malaysia is categorized into two types: Northeast Monsoon (NEM) and Southwest Monsoon (SWM), occurring from November to February and late May to August, respectively [18]. In comparison, the SWM season was much drier than NEM. Cold surge phenomena occurred throughout the NEM season, which is associated with higher intensity and prolonged precipitation, leading to increased river discharge and runoff from the land. When combined with high tides and strong onshore winds, the potential for storm surges during this period becomes significantly critical.


**Fig. 2** *Research area focusing on peninsular Malaysia, exposed directly to the South China Sea*

Aside from the monsoon phenomenon, Malaysia is also influenced by the El Niño and La Niña climate pattern events, resulting from variations in ocean temperature [19]. In Malaysia, El Niño was referred to as El Niño-Southern Oscillation (ENSO) resulting in sea level falls and La Niña resulting in sea level rise [20]. This event has altered the pattern of storm surge characteristics on the coastline. During La Niña, the sea surface temperatures in the central and eastern Pacific Ocean become cooler than usual which leads to different atmospheric circulation patterns and NEM becomes more active. It brings along a stronger northeasterly winds and higher precipitation to the eastern regions of Malaysia which calls for anticipation towards mitigating the impacts on coastal communities and infrastructure.

Prioritizing the understanding of the local weather pattern, this study focuses on the NEM period. Four different locations, including Geting (GT), Chendering (CD), Kuala Pahang (KP), and Tanjung Sedili (TS), were selected from each state on the East Coast of Peninsular Malaysia, with specific coordinates shown in Table 1 and Fig. 3.

**Table 1** *Observation stations within study area*

| Name of Stations | Code | Location |
|---|---|---|
| Geting | GT | $6.23°N, 102.10°E$ |
| Chendering | CD | $5.27°N, 103.18°E$ |
| Kuala Pahang | KP | $3.533°N, 103.55°E$ |
| Tanjung Sedili | TS | $1.917°N, 104.18°E$ |

Int. Journal of Integrated Engineering Vol. 16 No. 1 (2024) p. 394-410

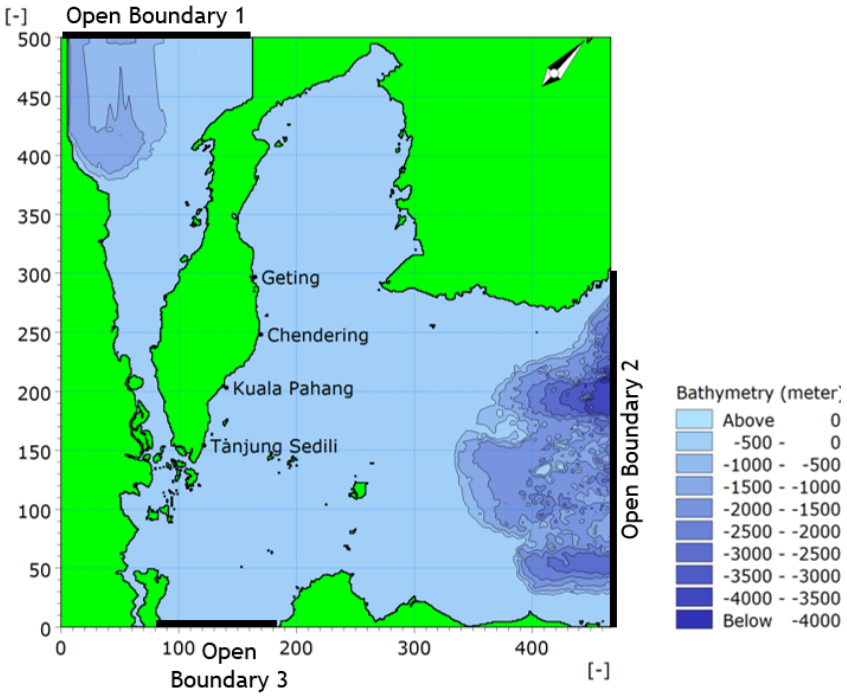


**Fig. 3** *Observation stations in East Coast of Peninsular Malaysia with open boundaries in model setup*

## 2.3 Storm Surge Simulation Setup

A total of three simulation phases involved with two parameters of data used in this research including the sea level pressure (SLP) and wind data. Wind data could be further separated into two components - UAOPN (east-west) and VAOPN (north-south) that represent the direction of wind or zonal components of the wind velocity. The data are available in binary format and were processed using a MATLAB program and a Python script, developed specifically for this study, to extract the SLP and wind velocities for a specific set of coordinates. The data was then input into a 3D matrix to allow for gridded interpolation to extract out the met-ocean data based on a separate set of coordinates and time points that could suit MIKE 21HD format.

The model used for this research is the MIKE 21 Flow Model in MIKE 21HD, which allows users to simulate water flow and water level variations in rivers, estuaries, coastal, and open sea areas. The FM model solves the Navier-Stokes equations that govern fluid flow using numerical algorithms and can be calibrated and validated using field measurements and satellite observations. The focus was narrowed down to selecting the hydrodynamic module, aligning with the parameters chosen for this study. To discretize the study area and facilitate the modelling process, a structured mesh approach was employed. This involved dividing the study area into a regular grid with fixed and uniform resolution. The structured mesh approach offers higher stability for simulations compared to the flexible mesh approach, making it a suitable choice for this study. To represent the underwater terrain and water depths accurately, bathymetry data was generated from GEBCO (General Bathymetric Chart of the Oceans) and incorporated into the model with the help of ArcGIS. It was projected with UTM-48 map projection to ensure consistency and proper representation of the study area's geographical features.

To ensure the model's stability during simulations, the maximum Courant number (CFL) or Courant-Friedrichs-Lewy number was carefully managed, aiming for values below two. This dimensionless number is usually used in numerical simulation particularly in fluid dynamics, to ensure stability and accuracy of the solution. It should be high enough to capture dynamic changes accurately but not so high that it compromises numerical stability. Boundary conditions for the model were adjusted with three open boundaries, taking into consideration the resistance present and Smagorinsky constant value of 0.5 was applied. The choice of 0.5 indicates a moderate level of turbulence and mixing - a higher Smagorinsky constant would result in more turbulence and mixing, while a lower value would reduce these effects.

### 2.3.1 Phase 1: Selection of Ensemble

Sub-section The first phase began with the selection of the ensemble process, which is necessary, as a large number of ensembles would slow down the process model due to limitations in the size of data storage and computational resources [21]. It involved a four-step approach to assess the suitability of the ensemble member in representing observed climate changes.

Firstly, a comprehensive visualization and comparison were conducted to analyze the long-term trends of the ensemble member and juxtapose them with the observed data. This initial assessment aimed to ensure a coherent alignment between the model output and observed climate behavior. Subsequently, a meticulous data calibration step was implemented to rectify potential systematic disparities or biases. By applying bias correction or correction factors to the d4PDF data, it was possible to refine its alignment with the observed data, consequently bolstering reliability. Moving forward, a rigorous quantile-quantile (Q-Q) plot comparison was performed to evaluate the statistical distribution and inherent characteristics of the ensemble member. Lastly, return periods were calculated to gauge the frequency and severity of extreme climate events.

This comprehensive and structured four-step approach facilitated a robust evaluation and selection of the ensemble member, incorporating both long-term trends and statistical properties, thereby ensuring the credibility and dependability of subsequent climate data analyses and interpretations. The selected ensembles would then be used along with the observation data for model baseline and future scenarios simulation.

### 2.3.2 Phase 2: Model Baseline

In the simulation setup, calibration of the d4pdf data was performed to ensure accurate and reliable results. The selected d4pdf data and observation data were both imported into MIKE 21HD. In this phase, the d4PDF Present-day Experiment (HPB) data type was utilized as it represents the current climate conditions without any additional forcing from greenhouse gas emissions. It serves as a reference point for evaluating the potential impacts of future climate changes under each of the scenarios.

Using the data extraction FM tools in Mike 21HD, a direct comparison was made based on the coordinates of interest. The results were then reviewed using the plot composer tool in MIKE Zero. To calibrate the data, the root mean square error (RMSE) was used as a metric, aiming to achieve an error below 10%. Additionally, the calibration results were crosschecked with the findings from previous studies. If the data did not meet the desired calibration standard, adjustments were made to the boundary conditions and resistance parameters. Once the calibration criteria were satisfied, the simulations for other scenarios were conducted using the calibrated data.

### 2.3.3 Phase 3: Future Scenarios

For future simulations, the warming SLP and wind data were forced into the calibrated model. The SSHs for the selected future scenarios were calculated using the same method employed in the baseline simulation. By comparing the SSHs from the future simulations with the present data, the insights into the potential impacts of climate change on storm surges during the Northeast Monsoon (NEM) season in Malaysia is gained.

Due to time constraints and limited access to MIKE 21HD licenses, the study focuses on the NEM season, considering only a few months of simulation for a limited number of years. Although the simulation period is relatively short, the selected NEM events are essential as they represent critical weather patterns affecting the eastern regions of Malaysia.

## 3. Results and Analysis

## 3.1 Selection of Critical Ensemble

### 3.1.1 Step 1: Visualization and Comparison

The aim of this step was to identify the ensemble member that exhibits the closest resemblance to the observed data in terms of its distribution characteristics. This identification serves as the initial subset of ensembles that will undergo further analysis in subsequent steps of the ensemble selection process. In this step, all ensemble members are plotted on a single graph alongside the observation data. The distributional patterns, the shape of the data, and the variability were examined separately for windspeed and SLP. As the windspeed came in the components of UAOPN and VAOPN, the windspeed is calculated before the data plotting was conducted. Data was represented using the Probability Density Function (PDF), a valuable statistical tool for understanding the distribution of continuous random variables and estimating probabilities. The PDF was also used to derive the mean and standard deviation aside from visualization and comparison as shown in Fig. 4 and Fig. 5.

Int. Journal of Integrated Engineering Vol. 16 No. 1 (2024) p. 394-410

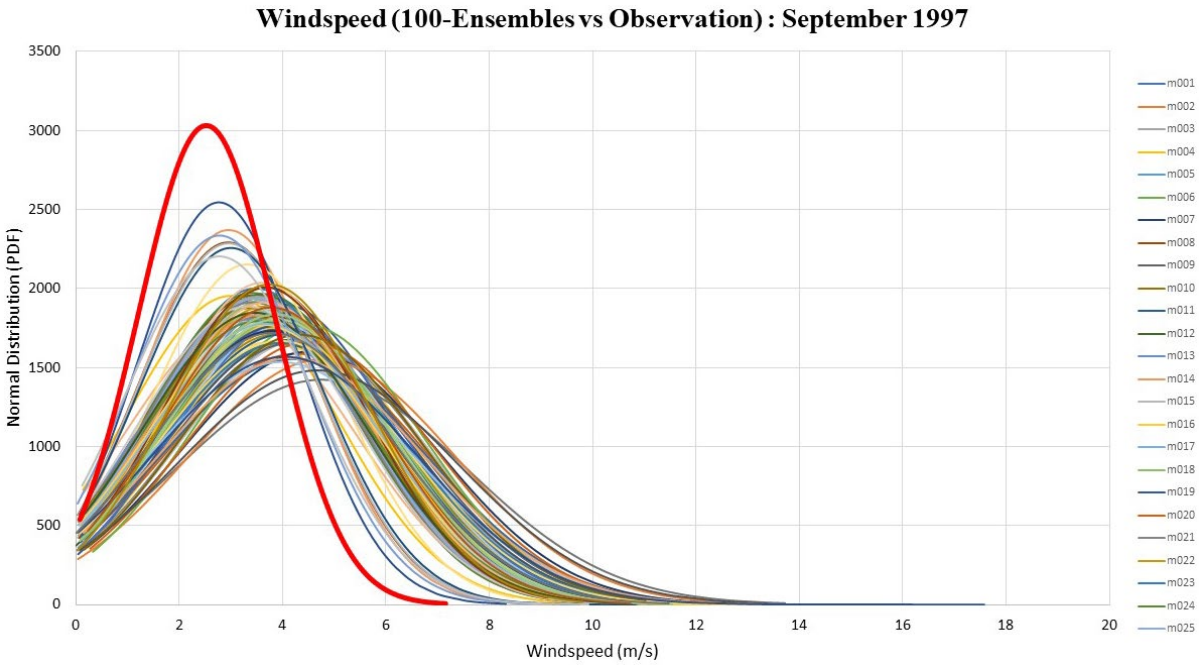


**Fig. 4** *Visualization of d4PDF-windspeed against observation data*

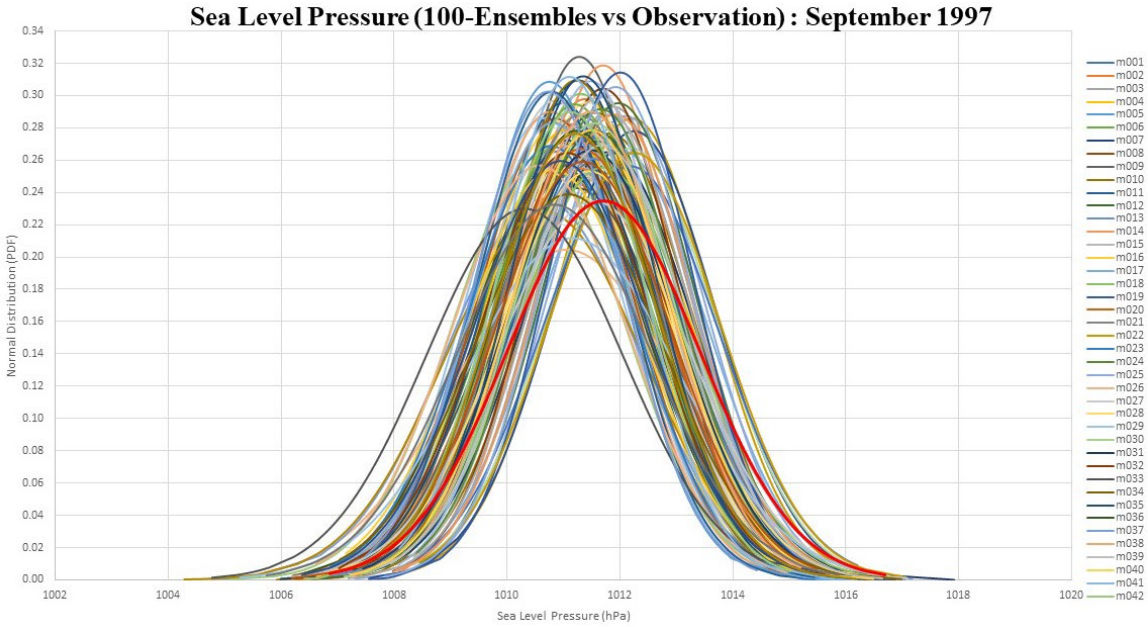


**Fig. 5** *Visualization of d4PDF-sea level pressure against observation data*

From this process, the selected ensembles include past wind speeds (m043), +2K wind speeds (m101), and +4K wind speeds (m111). As for the SLP, past sea level pressure (m099), +2K sea level pressure (m101), and +4K sea level pressure (m108) had been chosen as critical inputs for the future simulations.

### 3.1.2 Step 2: Data Calibration

The selected ensembles were then plotted alone against the observation data. The objective of this step was to align the selected ensemble member more closely with the observed data. The mean and standard deviation of ensembles were then compared with those of the observation data.

Examining these properties helps identify any systematic differences or biases between the ensemble member and the observed data. The correction factors were then applied to d4PDF data to displace and fit in the observation data as shown in Fig. 6. This process is repeated for all selected ensembles and applied to both windspeed and SLP.

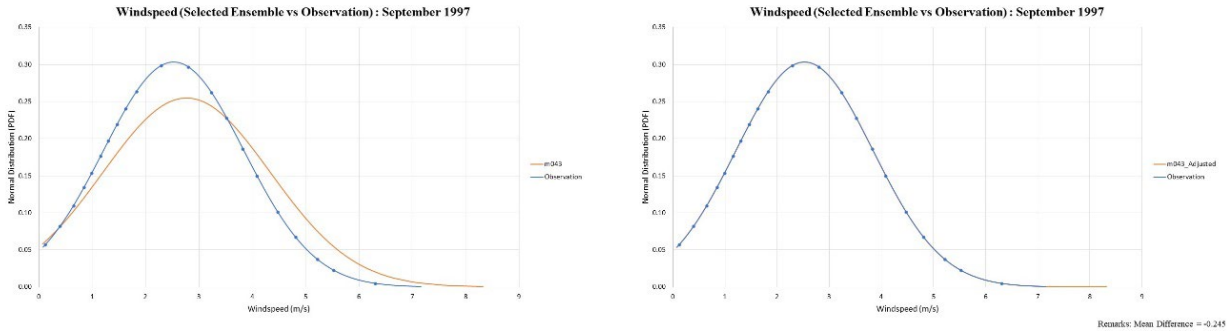


**Fig. 6** *Bias correction of data for selected ensemble*

### 3.1.3 Step 3: Q-Q Plot Comparison

The Q-Q plot (Quantile-Quantile plot) is a graphical technique used to compare the quantiles of two datasets. In this case, it involves plotting the quantiles of the observed data against the quantiles of the calibrated ensemble data in order to assess the conformity of calibrated and theoretical normal distribution as shown in Fig. 7.

Aiming to mitigate the deviation in the Q-Q plot trendline, a 45-degree line (slope=1) was constructed to be set as a benchmark. If the data points fall below the 45-degree line, it means that the sample data has lower quantiles (smaller values) compared to the theoretical distribution, indicating that the sample data has heavier tails or more spread out than the theoretical distribution. This suggested that the sample data is more closely packed around the mean compared to the theoretical distribution.

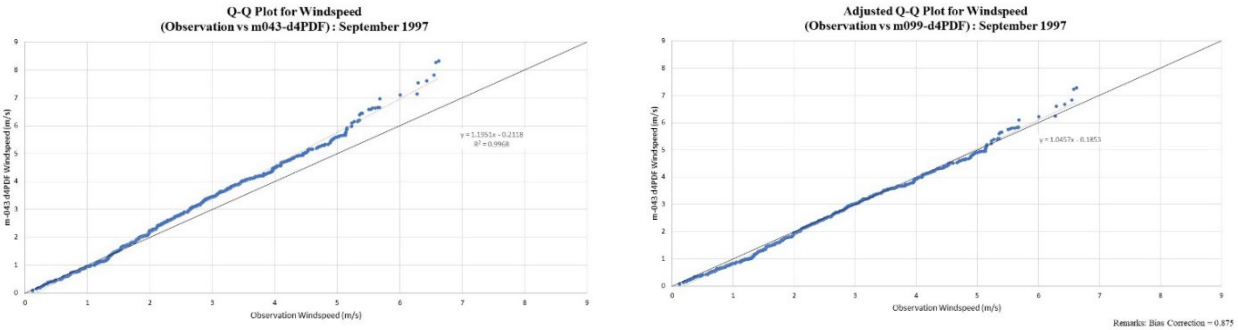


**Fig. 7** *The Q-Q plot and its adjustment for windspeed dataset*

Conversely, if the data points fall above the 45-degree line, it means that the sample data has higher quantiles (larger values) compared to the theoretical distribution, indicating that the sample data has lighter tails or is more concentrated around the mean than the theoretical distribution. Regarding windspeed in Fig. 7, the sample data has more extreme values and is adjusted towards the 45-degree line.

### 3.1.4 Step 4: Return Period Calculation

The calculation of return periods involved determining the probability of an event of a certain magnitude or threshold being exceeded in a given time period. The data was sorted in ascending order, and a threshold level was defined to identify extreme events. The return period was estimated using the formula $(N + 1)/(R + 1)$, where N is the total number of data points and R is the rank of the threshold level. This provided an average time between events of similar magnitude. While this approach offers initial insights, it assumes a stationary probability distribution. Nonetheless, the return periods were calculated for all ensemble to determine the maximum, average and minimum values for future scenarios as shown in Fig. 8.

Int. Journal of Integrated Engineering Vol. 16 No. 1 (2024) p. 394-410

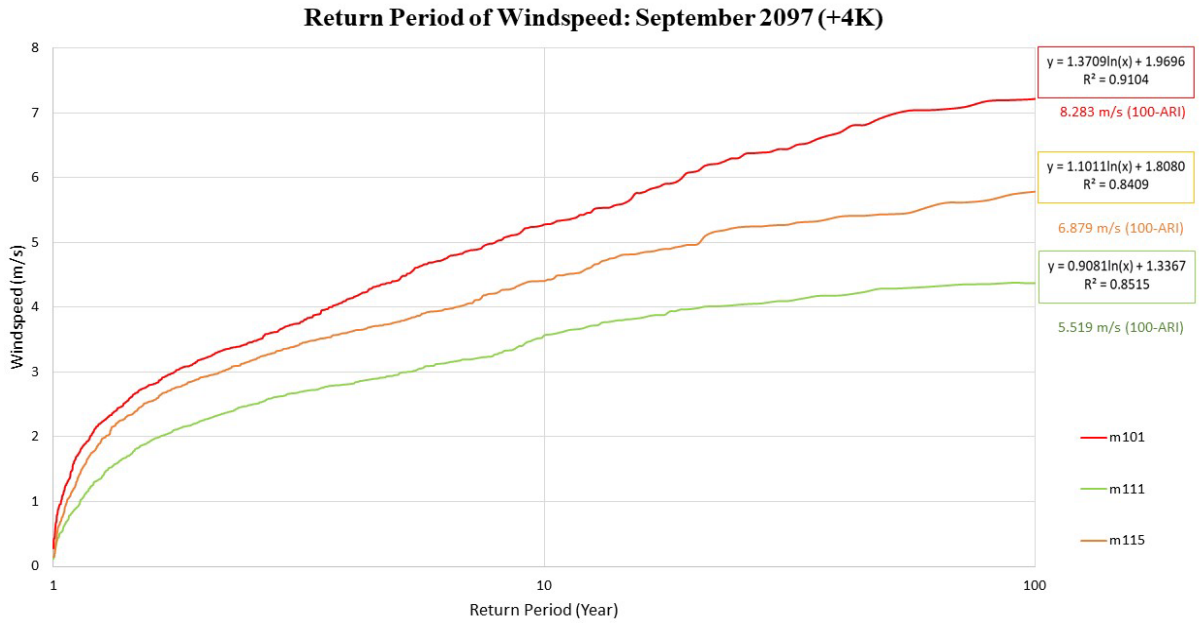


**Fig. 8** *Calculation of return period for selected ensembles*

## 3.2 Modelling Baseline

From the analysis of selected ensembles, the raw data was converted and transferred into MIKE21 HD format. The converted wind and SLP datasets were shown in Fig. 9 and Fig. 10. The simulation involved running scenarios with and without wind conditions to obtain the modeled tidal elevation.

The Root Mean Square Error (RMSE) calculation was then applied, serving as a statistical measure to quantify the divergence between predicted and actual variable values. It is widely employed in regression analysis for assessing the precision of a predictive model. The observed tidal level (represented in graph as predicted tidal level) was plotted against modelled tidal level of d4PDF HPB data as shown in Fig. 11.

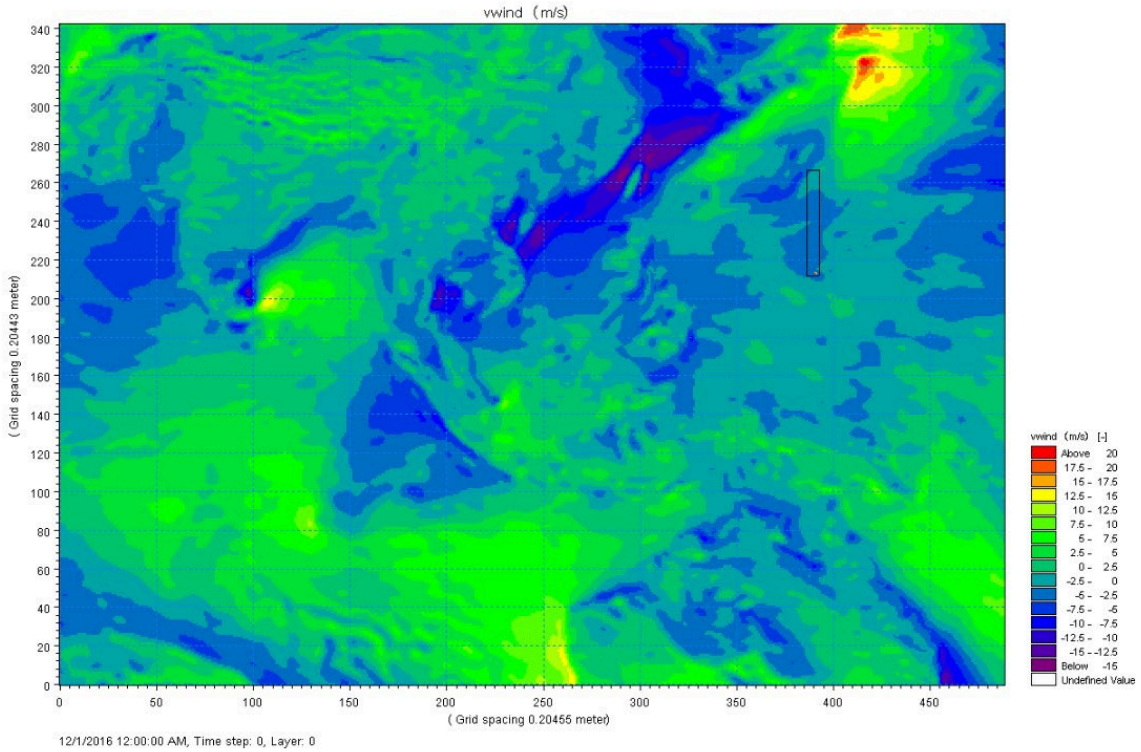


**Fig. 9** *Converted wind-d4PDF dataset into MIKE 21HD format*

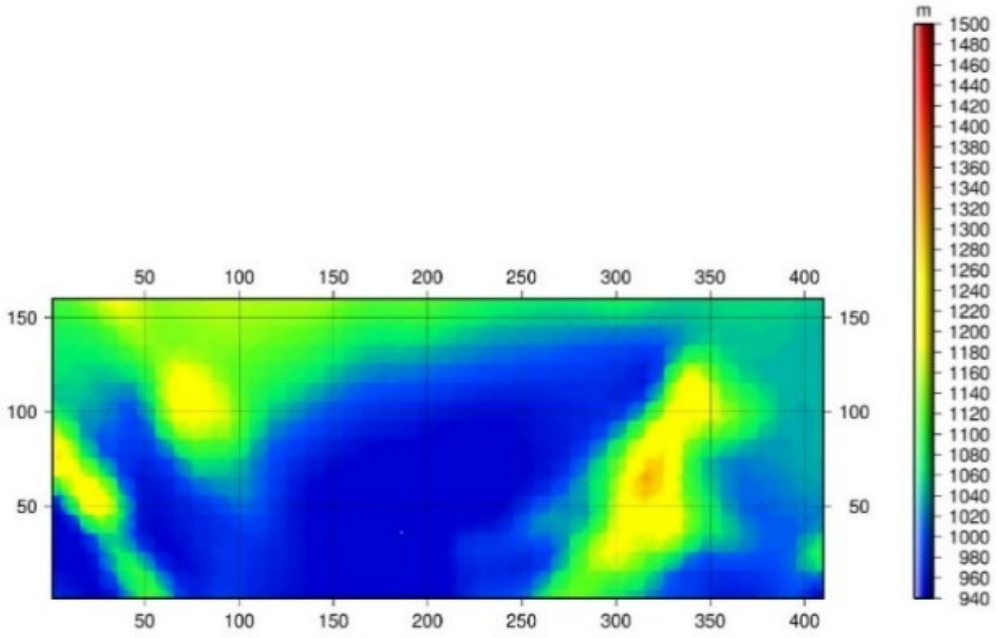


**Fig. 10** *Converted SLP-d4PDF data into MIKE 21HD format*

Int. Journal of Integrated Engineering Vol. 16 No. 1 (2024) p. 394-410

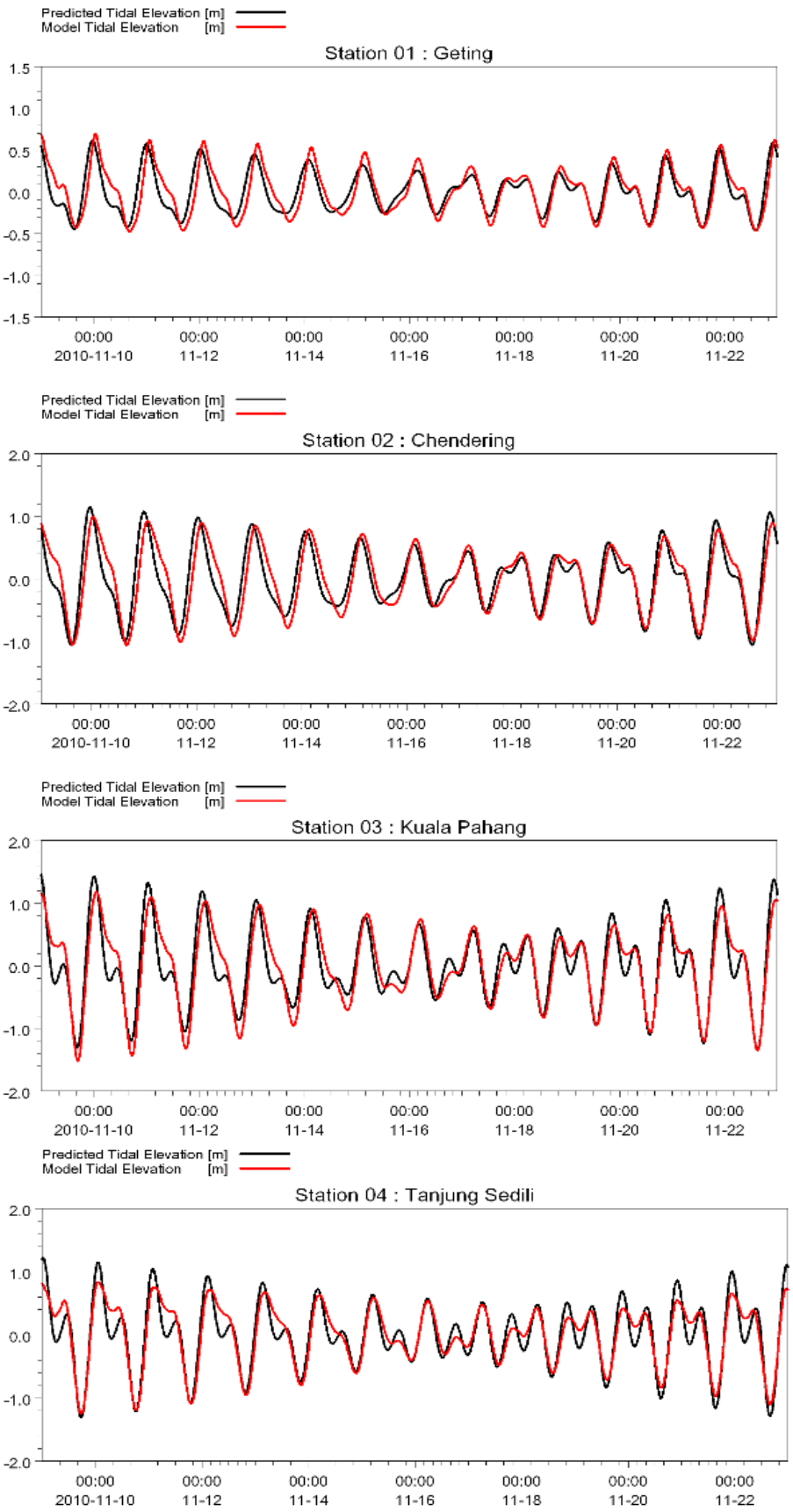


**Fig. 11** *Tidal elevation comparison between modelled and observed datasets*

Table 2 displays the RMSE values obtained for each station, indicating the accuracy of the model's predictions compared to the observed data.

**Table 2** *RMSE calculation at each station*

| Ref | Station Name | RMSE (%) |
|---|---|---|
| 1 | Geting | 13.37 |
| 2 | Chendering | 10.95 |
| 3 | Kuala Pahang | 8.98 |
| 4 | Tanjung Sedili | 7.27 |

For the station "Geting," the RMSE value of 13.37% suggested that the model's predictions have an average error of 13.37% compared to the observed data. Similarly, for the station "Chendering," the RMSE value of 10.95% represents an average error of 10.95%. Both stations show reasonably good agreement between the model and the observed data.

The station "Kuala Pahang" exhibits a lower RMSE value of 8.98%, revealed a higher accuracy of the model in predicting the SSH at this location. Lastly, the station "Tanjung Sedili" has the lowest RMSE value of 7.27%, representing the closest match between the model predictions and the actual observations.

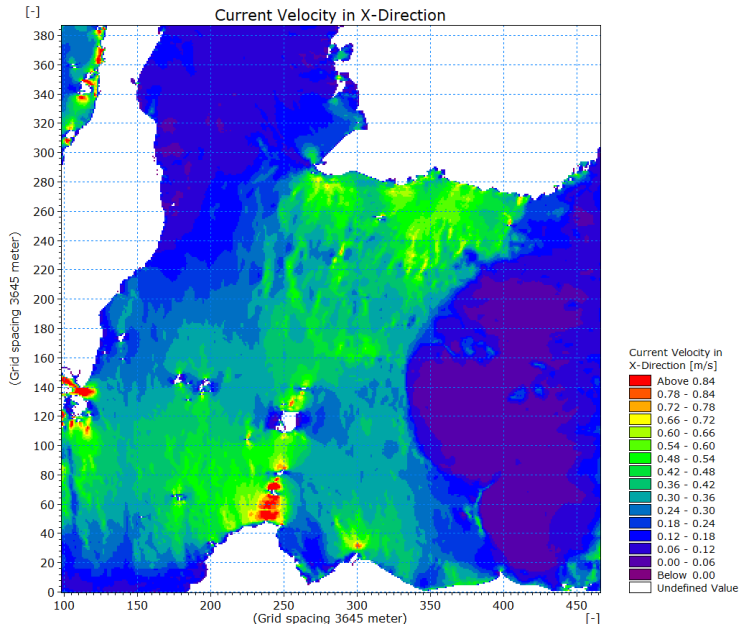


**Fig. 12** *Current velocity in X-direction*

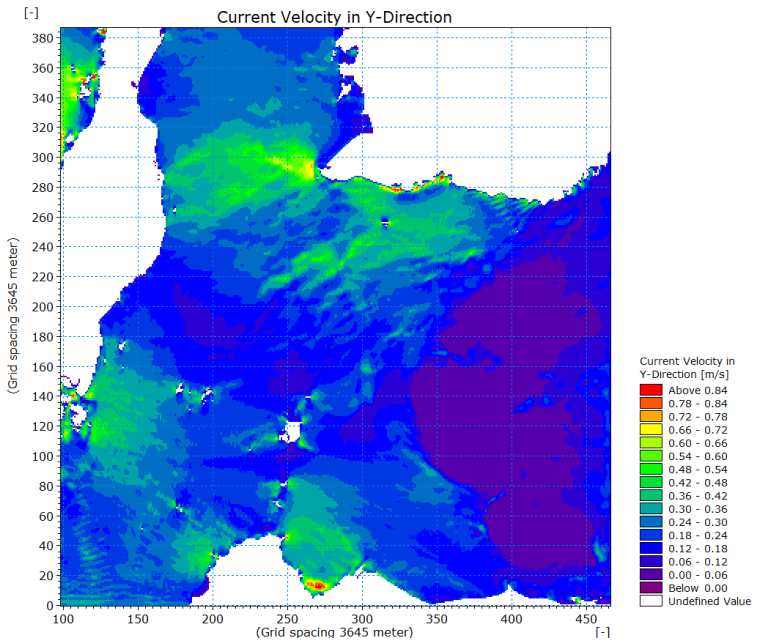


**Fig. 13** *Current velocity in Y-direction*

Int. Journal of Integrated Engineering Vol. 16 No. 1 (2024) p. 394-410

Overall, the lower RMSE values for all stations demonstrate the effectiveness of the MIKE 21 flow model in simulating SSH accurately. As the RMSE fell within acceptable range, hindcast and forecast simulation were conducted. From the output, the maximum current velocity was extracted in X and Y direction as shown in Fig. 12 and Fig. 13. In the current velocity in X-Direction, colors shift from dark purple to red, representing different strengths of east-west currents. Similarly, the current velocity in Y-Direction uses a color spectrum to illustrate variations in north-south current velocities. Warmer colors indicate higher speeds.

MIKE 21HD is capable of providing the current speed as well. Fig. 14 displays the plot for maximum current speed, which varies depending on factors such as tidal cycles, seasonal weather patterns, and ocean currents.

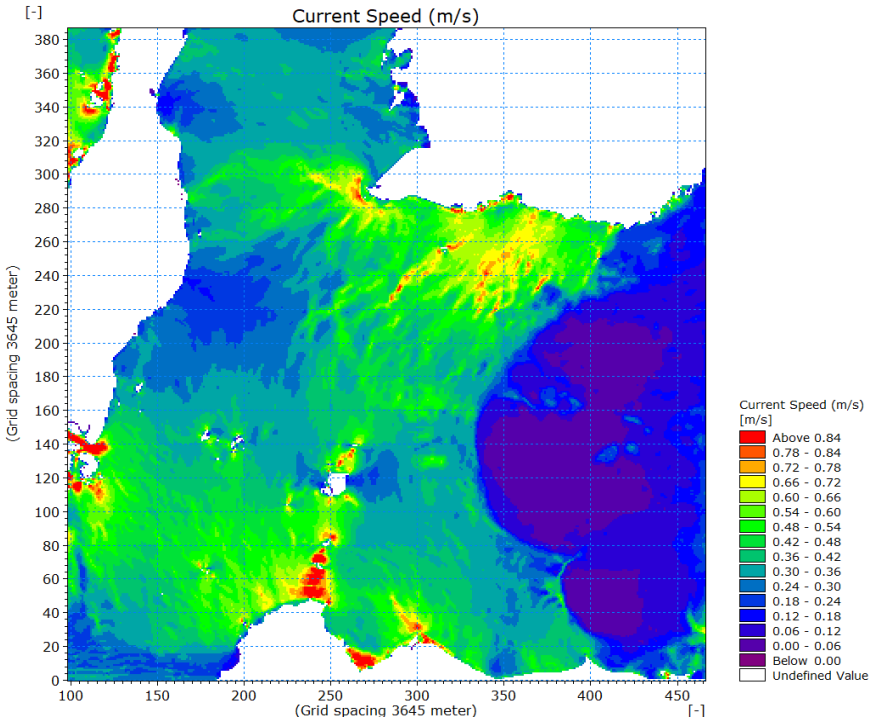


**Fig. 14** *Current speed around study area*

## 3.3 Simulation Analysis: +2K and +4K Scenarios

To compute the surge heights, the predicted tide was subtracted from the observed tide gauge data for each station during a specified timeframe. For this analysis, the duration was limited to the period between November to March, encompassing the northeast monsoon (NEM) season, spanning a total of five months.

- Scenario 1 (past data): 2010 to 2011
- Scenario 2 (future data): +2K climate change for year 2090 to 2091
- Scenario 3 (future data): +4K climate change for year 2090 to 2091

Fig. 15 illustrates the comparison between three distinct scenarios where the graphs indicate that a rise in temperature is correlated with an increase in SSH. The data consistently demonstrates that the +4K climate change datasets produce surge height readings that are higher than those of the +2K datasets.

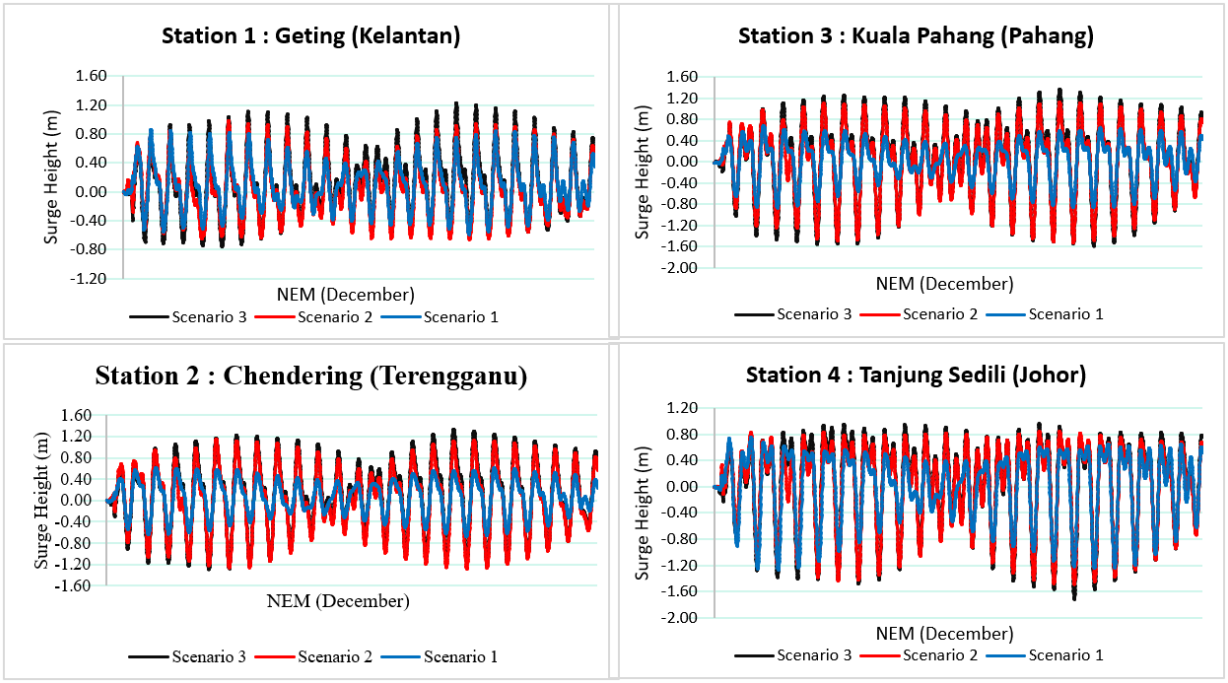


**Fig. 15** *Comparison for past and future (2K and 4K) climate change scenarios*

Apart from current speed, MIKE 21HD also has the capability to identify the maximum surge height, which is illustrated in Fig. 16. The values obtained from the output were extracted and presented in tabular form, as depicted in Table 3.

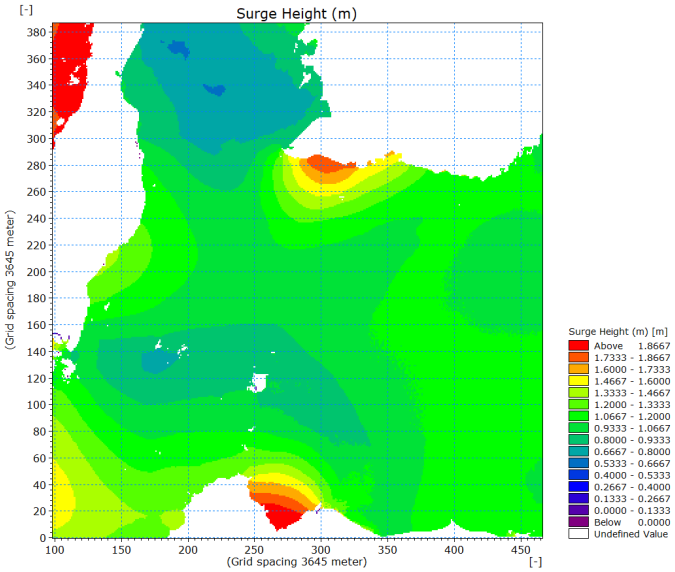


**Fig. 16** *Maximum surge height identification*

**Table 3** *Maximum surge heights at each station*

| Station | Maximum Surge Heights (m) | | |
|---|---|---|---|
| | Scenario 1 (Past: 2010 to 2011) | Scenario 2 (Future: +2K Climate Change) | Scenario 3 (Future: +4K Climate Change) |
| Geting | 0.852 | 1.035 | 1.251 |
| Chendering | 0.619 | 1.167 | 1.344 |
| Kuala Pahang | 0.683 | 1.159 | 1.379 |
| Tanjung Sedili | 0.888 | 1.039 | 1.089 |

Based on the presented data, it is apparent that SSHs are projected to increase for all stations under future climate scenarios (+2K and +4K) in comparison to the past scenario. The rise in surge height for all stations is in line with the temperature increase observed in the +2K and +4K scenarios. Furthermore, the results indicate that the surge height increment is directly proportional to the temperature increase, with higher temperature increases resulting in higher surge heights. In comparing the +2K and +4K scenarios, it is evident that the SSH increment is more significant in the +4K scenario than in the +2K scenario for all stations. This is expected since the temperature increase is more severe in the +4K scenario compared to the +2K scenario.

For Geting in Kelantan, the SSH projection is expected to rise from 0.852m in the past scenario to 1.035m and 1.251m in the +2K and +4K scenarios, respectively. For Chendering in Terengganu, the SSH projection is expected to increase from 0.619m in the past scenario to 1.167 m and 1.344 m in the +2K and +4K scenarios, respectively. Similarly, for Kuala Pahang in Pahang, the SSH projection is expected to increase from 0.683m in the past scenario to 1.159m and 1.379m in the +2K and +4K scenarios, respectively. In contrast, Tanjung Sedili in Johor is the only station with a slight decrease in SSH projection to 1.039 m and 1.089 m in the +2K and +4K scenarios, respectively.

A comparison between stations reveals that the SSH projections are higher in the east coast of Peninsular Malaysia, particularly in Kelantan and Terengganu, with a projected increase of up to 0.725m in the +2K and +4K scenarios. Pahang also shows a significant increase in the SSH projections, with a projected increase of up to 0.696m in the +2K and +4K scenarios. In contrast, Johor is the only station with a slight decrease in the SSH projection in the +2K and +4K scenarios.

The direct proportionality between temperature increases and surge height increments, observed in our study, aligns with the historical trends identified by Anuar et al. [20], thereby strengthening the temporal correlation between climate dynamics and storm surge occurrences. The study spans a period from 1986 to 2013 and observes a decline in surge levels in the late 90s, followed by a gradual increase, aligning with our projection of future SSH scenarios (+2K and +4K). The observed pattern of increment is consistent with the current understanding of climate change's impacts on SSH. The higher sea surface temperatures projected in the future scenario contribute to increased evaporation and moisture content in the atmosphere, leading to more intense storms and higher SSHs. These changes contribute to an elevated storm surge risk along the coastal areas, especially when combined with other factors like heavy rainfall, strong winds, and high tide.

SSHs can be considered dangerous depending on various factors such as the topography, coastal infrastructure, and population density of the affected areas. The provided data does not explicitly indicate the danger level of these SSHs. It is crucial to assess the vulnerability and resilience of the coastal areas and their preparedness to handle such events. To determine the significance of the SSHs, further analysis is required, including the local coastal conditions, land use patterns, and potential impacts on human settlements, ecosystems, and infrastructure.

## 4. Conclusion

In conclusion, this study utilized the MIKE 21 flow model and data from the d4PDF database to investigate the impacts of climate change on SSH in coastal areas of Malaysia. Numerical validation through RMSE and LR analysis confirmed the accuracy of the model and the reliability of the d4PDF data in addressing climate change scenarios.

During the northeast monsoon (NEM) duration, the analysis revealed a consistent trend where the SSH (SSH) increment correlated with the increment of temperature. The future climate scenarios of +2K and +4K demonstrated significant increases in SSH compared to the past baseline period. The findings highlight the potential risks and challenges posed by climate change on coastal regions, especially during NEM events.

The results of this study are crucial for coastal management and planning in Malaysia. By providing valuable insights into the impacts of climate change on SSH, policymakers, urban planners, and coastal communities can make informed decisions and implement effective adaptation strategies to mitigate the potential consequences. By recognizing the alignment between SSH increment and temperature increase, stakeholders can take proactive steps to address the challenges posed by rising SSHs and safeguard the coastal communities and ecosystems of Malaysia from the impacts of climate change.

## Acknowledgement

The authors would like to thank Dr Nik & Associates Sdn Bhd for the provision of the MIKE 21HD model, and the data required for this study. This research was funded by the Murata Science Foundation (21MP04) and YUTP-FRG Grant (015LC0-453)

## Conflict of Interest

Authors declare that there is no conflict of interests regarding the publication of the paper.

## Author Contribution Statement

*The authors confirm contribution to the paper as follows:* ***study conception and design:*** *Teh Hee Min, Nurdiyana Nabilah Rosli, Kim Sooyoul;* ***data collection:*** *Nurdiyana Nabilah Rosli, Kim Sooyoul;* ***analysis and interpretation of results:*** *Nurdiyana Nabilah Rosli, Teh Hee Min, Kim Sooyoul;* ***draft manuscript preparation:*** *Nurdiyana Nabilah Rosli, Teh Hee Min. All authors reviewed the results and approved the final version of the manuscript.*

## References

[1] Rahman, H. A. (2018). Climate change scenarios in Malaysia: engaging the public. International Journal of Malay-Nusantara Studies, 1(2), 55-77.
[2] World Bank Group (2021). Climate Risk Country Profile. Washington, pp. 1-28.
[3] Kang, S., Im, E. S., & Eltahir, E. A. B. (2019). Future climate change enhances rainfall seasonality in a regional model of western Maritime Continent. Climate Dynamics, 52(1), 747-764. https://doi.org/10.1007/s00382-018-4164-9
[4] Raghavan, S. V., Vu, M. T., & Liong, S. Y. (2017). Ensemble climate projections ofmean and extreme rainfall over Vietnam. Global and Planetary Change, 148, 96-104. https://doi.org/10.1016/j.gloplacha.2016.12.003
[5] Thanh, N. D., Kieu, C., Thatcher, M., Dzung, N. L., & Tan, P. V. (2014). Climate projections for Vietnam based on regional climate models. Climate Research, 60, 199-213. https://doi.org/10.3354/cr01234
[6] Manomaiphiboon, K., Octaviani, M., Torsri, K., & Towprayoon, S. (2013). Projected changes in means and extremes of temperature and precipitation over Thailand under three future emissions scenarios. Climate Research, 58, 97-115. https://doi.org/10.3354/cr01188
[7] IPCC (2014). Climate Change 2014. Synthesis Report, Contribution of Working Groups I, II and III to the Fifth Assessment Report of the Intergovernmental Panel on Climate Change, pp. 155.
[8] Dasgupta, S., Laplante, B., Murray, S., & Wheeler, D. (2011). Climate change and the future impacts of storm-surge disasters in developing countries. SSRN Electronic Journal, 182. https://doi.org/10.2139/ssrn.1479650
[9] Awang, N. A., & Hamid, M. R. (2013). Sea level rise in Malaysia. Hydrolink, 2, 47-49.
[10] Razali, A. M., Sapuan, M. S., Ibrahim, K., Zaharim, A., & Sopian, K. (2010). Mapping of annual extreme wind speed analysis from 12 stations in Peninsular Malaysia. International conference on System Science and Simulation in Engineering, Japan, pp. 397-403.
[11] Kim. S. (2019). Storm Surges. Encylopedia of Ocean Sciences, pp. 663-670. http://dx.doi.org/10.1016/B978-0-12-409548-9.10849-8
[12] Mizuta, R., Murata, A., Ishii, M., Shiogama, H., Hibino, K., Mori, N., Arakawa, O., Imada, Y., Yoshida, K., Aoyagi, T., Kawase, H., Mori, M., Okada, Y., Shimura, T., Nagatomo, T., Ikeda, M., Endo, H., Nosaka, M., Arai, M., Takahashi, C., Tanaka, K., Takemi, T., Tachikawa, Y., Temur, K., Kamae, Y., Watanabe, M., Sasaki, H., Kitoh, A., Takayabu, I., Nakakita, E., & Kimoto, M. (2017). Over 5,000 years of ensemble future climate simulations by 60-km global and 20-km regional atmospheric models. Bulletin of the American Meteorological Society, 98(7), 1383-1398.
[13] Tanaka, T., Kobayashi, K., & Tachikawa, Y. (2021). Simultaneous flood risk analysis and its future change among all the 109 class-A river basins in Japan using a large ensemble climate simulation database d4PDF. Environmental Research Letter, 16(7), 1-12. https://doi.org/10.1088/1748-9326/abfb2b
[14] Sato, T., & Nakamura, T. (2019). Intensification of hot Eurasian summers by climate change and land–atmosphere interactions. Scientific Reports, 9(1), 1-8. https://doi.org/10.1038/s41598-019-47291-5
[15] Yamada, T. J., & Hoshino, T. (2020). The analysis of future flood risk in Hokkaido, Northern Japan, using database for policy decision making for future climate change (d4PDF). Proceedings of the 22nd IAHR APD Congress.
[16] Kanada, S., Tsuboki, K., & Takayabu, I. (2020). Future changes of tropical cyclones in the midlatitudes in 4-km-mesh downscaling experiments from large-ensemble simulations. Scientific Online Letters on the Atmosphere, 16, 57-63. https://doi.org/10.2151/sola.2020-010
[17] Watanabe, S., Yamada, M., Abe, S., & Hatono, M. (2020). Bias correction of D4PDF using a moving window method and their uncertainty analysis in estimation and projection of design rainfall depth. Hydrological Research Letters, 14(3), 117–122. https://doi.org/doi: 10.3178/hrl.14.117
[18] Suhaila, J., Deni, S. M., Zawiah, W. A. N., & Jemain, A. A. (2010). Trends in Peninsular Malaysia rainfall data during the southwest monsoon and northeast monsoon seasons: 1975-2004. Sains Malaysiana, 39(4), 533–542.
[19] Kamil, N. N., & Omar, S. F. (2017). The impact of El Niño and La Niña on Malaysian palm oil industry. Oil Palm Bulletin, 74, 1-6.

Int. Journal of Integrated Engineering Vol. 16 No. 1 (2024) p. 394-410

[20] Anuar, N. M., Hashim, A. M., Awang, N. A., & Hamid, M. R. A. (2018). Historical storm surges: Consequences on coastal resources and shoreline protection in the East Coast of Peninsular Malaysia. Daniel Bung, Blake Tullis, 7th IAHR International Symposium on Hydraulic Structures, Aachen, Germany, 15-18 May. doi: 10.15142/T33H1T (978-0-692-13277-7).
[21] Ishii, M., & Mori, N. (2020). d4PDF: large-ensemble and high-resolution climate simulations for global warming risk assessment. Prog Earth Planet Sci 7, 58. https://doi.org/10.1186/s40645-020-00367-7.